



Frost resistance of concrete with high contents of fly ash - A study on how hollow fly ash particles distort the air void analysis

Hasholt, Marianne Tange; Christensen, Katja Udbye; Pade, Claus

Published in:
Cement and Concrete Research

Link to article, DOI:
[10.1016/j.cemconres.2019.02.013](https://doi.org/10.1016/j.cemconres.2019.02.013)

Publication date:
2019

Document Version
Early version, also known as pre-print

[Link back to DTU Orbit](#)

Citation (APA):
Hasholt, M. T., Christensen, K. U., & Pade, C. (2019). Frost resistance of concrete with high contents of fly ash - A study on how hollow fly ash particles distort the air void analysis. *Cement and Concrete Research*, 119, 102-112. DOI: [10.1016/j.cemconres.2019.02.013](https://doi.org/10.1016/j.cemconres.2019.02.013)

General rights

Copyright and moral rights for the publications made accessible in the public portal are retained by the authors and/or other copyright owners and it is a condition of accessing publications that users recognise and abide by the legal requirements associated with these rights.

- Users may download and print one copy of any publication from the public portal for the purpose of private study or research.
- You may not further distribute the material or use it for any profit-making activity or commercial gain
- You may freely distribute the URL identifying the publication in the public portal

If you believe that this document breaches copyright please contact us providing details, and we will remove access to the work immediately and investigate your claim.

This is a preprint of an article published in Cement and Concrete Research:

Marianne Tange Hasholt, Katja Udbye Christensen, Claus Pade:

“Frost resistance of concrete with high contents of fly ash - A study on how hollow fly ash particles distort the air void analysis”

Cement and Concrete Research 119 (2019) 102–112

The published version is available online:

<https://doi.org/10.1016/j.cemconres.2019.02.013>

1 FROST RESISTANCE OF CONCRETE WITH HIGH CONTENTS OF FLY ASH - A STUDY
2 ON HOW HOLLOW FLY ASH PARTICLES DISTORT THE AIR VOID ANALYSIS

3

4 Marianne Tange Hasholt, Katja Udbye Christensen, and Claus Pade

5

6 **Abstract**

7 Cenospheres are hollow fly ash particles. When performing air void analysis on a contrast enhanced
8 plane section, air inclusions in cenospheres are counted as air voids. In the present study, air void
9 analyses for air entrained concrete mixtures with fly ash (up to 50% of binder mass) were corrected
10 based on chord counting for non-air entrained paste samples with various contents of fly ash. The
11 correction only lead to a small reduction of the total air content, but it increased the spacing factor
12 up to 25%. The concrete mixtures were also exposed to salt frost scaling testing. The amounts of
13 scaling were unacceptable for several mixtures with high dosages of fly ash. Inferior strength or
14 inadequate air void structure could not explain this. Additional testing pointed to that chemical
15 surface degradation aggravated the physical frost attack for concrete mixtures with high contents of
16 fly ash.

17

18 **1. Introduction**

19 Fly ash has been used in concrete production for many years [1]. There are economic,
20 environmental as well as technological reasons to substitute part of the cement with fly ash. For
21 example, fly ash addition reduces heat development at early age [2], and there is evidence that fly
22 ash addition can reduce chloride ingress, thereby making reinforced concrete structures more
23 durable [3].

24

25 Typically, the fly ash dosage in structural concrete is moderate, i.e. 15-25% of the binder content
26 [1]. However, recent years increasing awareness of the environmental impact of concrete
27 production has promoted a demand for concrete with higher fly ash dosages, as increased fly ash
28 addition is one way to lower the cement content and thereby the carbon footprint of concrete.

29

30 Salt frost scaling resistance seems to be a weak point for concrete produced with high volumes of
31 fly ash, where fly ash constitutes e.g. 50% of the binder. There are many studies documenting that
32 the salt frost scaling resistance of concrete with cement as the only powder is superior to the salt
33 frost scaling resistance of concrete with fly ash. However, in many of the studies, it can be argued
34 that concrete with and without fly ash are not compared on an equal footing:

35

- 36 • The concrete mixtures have the same water/binder ratio (W/B), i.e. fly ash replaces cement on a
37 1:1 mass basis. This procedure results in fly ash mixtures with lower strength than the reference
38 mixtures based on pure cement [4].
- 39 • The concrete mixtures are air entrained, and the dosage of air-entraining admixture (AEA) is
40 adjusted to obtain approximately the same air content in the fresh concrete [4, 5]. Fly ash
41 normally contains small amounts of unburnt carbon that can adsorb the AEA, making it inactive
42 [6]. Therefore, concrete with fly ash typically needs a higher dosage of AEA than concrete
43 without fly ash to obtain the same amount of air in the fresh concrete. However, as shown by
44 Siebel [7], comparable total air contents is not a sufficient precondition for having comparable
45 air void structures. If the concrete mixtures also include (super)plasticizers in varying dosages,
46 concrete mixtures with identical air contents may have very different air void structures in terms
47 of specific surface of the air voids and spacing factor. Many of the studies on the effect of fly
48 ash addition on salt frost scaling do not include air void analysis of the hardened concrete, so it

49 is not possible to judge if the air void structures of the concrete mixtures will provide
50 comparable protection against frost attack.

- 51 • The concrete mixtures have the same age at the initiation of the salt frost scaling test. The
52 pozzolan reaction, where fly ash reacts to form gel solid, is much slower than the hydration of
53 cement. Most standardized salt frost scaling tests are initiated 14 or 28 days after casting, and
54 this is not enough for concrete with fly ash to reach its full potential as regards frost resistance.
55 The problem becomes larger, when the fly ash dosage increases. Both [8] and [9] show that the
56 salt frost scaling of concrete with high volumes of fly ash is reduced significantly, if the start of
57 the freeze/thaw exposure is postponed to 91 or 180 days after casting.
- 58 • The same curing procedure is used prior to the frost test, no matter if the concrete mixture
59 composition includes fly ash or not. The curing procedure after demoulding normally consists of
60 a moist curing period (in water bath or fog room) and a drying period, where the concrete is
61 stored exposed to air with RH significantly lower than 100%, e.g. 50% or 65%. Ehrhardt [10]
62 showed that if using a relatively rapid hardening binder combination (2 days strength > 23 MPa,
63 where cement strength is measured according to EN 196-1), adequate salt frost scaling
64 resistance was obtained with a short moist curing period or even no moist curing at all. Slower
65 reacting binder combinations experienced harmful drying, resulting in poor surface quality, and
66 for this reason the concrete surface could not sustain a salt frost scaling test.

67

68 There are also studies showing that concrete with high volumes of fly ash, i.e. where fly ash
69 constitutes 50% or more of the binder, can possess adequate salt frost scaling resistance [11].

70 Concrete with high volumes of fly ash may be more sensitive to finishing and curing conditions, but
71 if the concrete work is carried out correctly, concrete with high volumes of fly ash has shown
72 excellent salt frost scaling resistance for e.g. pavements in service. For this reason, current best

73 practice for high-volume fly ash concrete do not advice against using the concrete in environments
74 where it is going to be exposed to frost and de-icing chemicals [12].

75

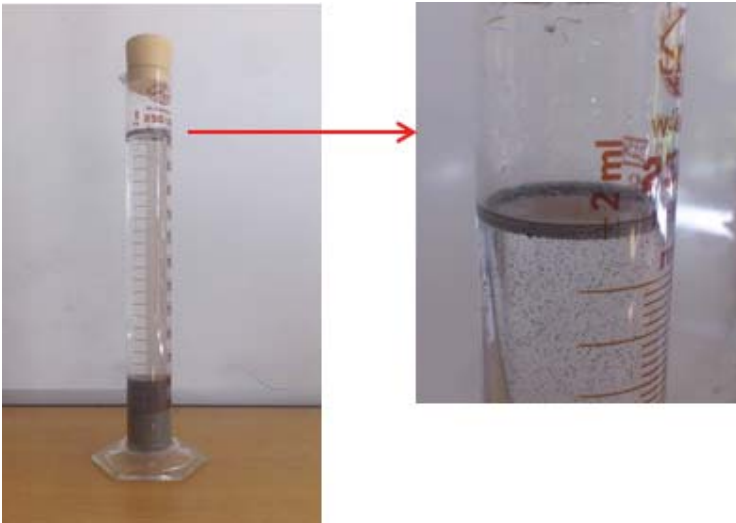
76 In a Danish development project “Green Transition of Cement and Concrete Production” aiming at
77 improving the environmental profile of concrete production, various properties were tested for
78 concrete, where fly ash made up 40-50% of the binder mass. Despite several attempts, none of the
79 mixtures passed an accelerated salt frost scaling test. The above-mentioned reasons for poor salt
80 frost scaling resistance could be discarded. The concrete mixtures with high contents of fly ash were
81 designed to have 28 days compressive strength comparable to a frost resistant reference mixture,
82 which had a much lower fly ash content. Therefore, the W/B was not fixed; the slower property
83 development of mixtures with high fly ash contents were compensated by lowering the W/B. The
84 dosage of AEA was also variable. Air void analysis of the hardened concrete showed that concrete
85 with high contents of fly ash fulfilled all requirements to frost resistant concrete, and e.g. the
86 spacing factor was on the same level as for the reference concrete. Last, the accelerated salt frost
87 scaling test was carried out on saw cut surfaces, so e.g. poor concrete surface quality would not
88 influence the result.

89

90 It was speculated that hollow fly ash particles would be counted as air voids in the air void analysis
91 without contributing to the frost resistance as entrained air voids, thereby making the outcome of
92 the air void analysis for concrete with high contents of fly ash misleading. Fly ash is a by-product
93 from coal combustion. At high temperatures, carbon and volatile matter burn, whereas mineral
94 impurities in the coal melt and form droplets. Fly ash particles are the cooled droplets, and they are
95 therefore spherical. Most of the fly ash particles are solid, but a small percentage is hollow particles

96 called cenospheres. The presence of cenospheres can easily be observed by suspending the fly ash
97 particles in water, see figure 1:

98



99 *Figure 1: When fly ash is suspended in water, the solid particles will settle at the bottom (left),*
100 *while the much lighter cenospheres gather at the water surface.*

101

102 In an air void analysis based on black and white color impregnation of a plane section, the empty
103 cavities of cenospheres will look like air voids. The error in the air void analysis is larger, the larger
104 the fly ash content. It was therefore decided to investigate if the presence of cenospheres could have
105 a significant effect on the outcome of the air void analysis. The investigation was carried out as part
106 of a Master thesis work at the Technical University of Denmark [13].

107

108 2. Materials and methods

109

110 2.1 Reference concrete

111 In Denmark, concrete requirements are a combination of prescriptive requirements and
112 performance-based requirements. According to DS 2426 [14] and the Danish Road Directorate's
113 standard specification for bridges, concrete exposed to severe freeze/thaw exposure (exposure class
114 XF4 according to EN 206 [15]) has to fulfill the following:

115

- 116 • Cement type: CEM I; minimum strength class: 42.5; sulfate resistance class: SR5 or better
- 117 • Maximum fly ash content: $FA/C = 0.33$ (i.e. $FA/(C+FA) = 0.25$)
- 118 • Maximum W/C_{eq} : 0.40 (according to DS 2426, fly ash content up to 33% of the cement content
119 can be taken into account by using an activity factor ($W/C_{eq} = W/(C+0.5 \cdot FA)$))
- 120 • Minimum strength class: C40/50
- 121 • Minimum air content in fresh concrete: 4.5%
- 122 • Frost resistance: The concrete has either passed an accelerated freeze/thaw test, or an air void
123 analysis of the hardened concrete has documented
 - 124 - air content in hardened concrete: 3.5% or higher
 - 125 - spacing factor in hardened concrete: 0.20 mm or lower

126

127 Concrete mixtures with high contents of fly ash ($FA/(C+FA) > 0.25$) cannot fulfill the prescriptive
128 requirement regarding maximum fly ash content. Typically, concrete mixtures with high contents of
129 fly ash are also challenged as regards maximum W/C_{eq} , as only a part of the fly ash is taken into
130 consideration when calculating the W/C_{eq} . This was one of the issues that initiated the development
131 project "Green transition of cement and concrete production". In this project, one of the goals is to

132 work towards purely performance-based specifications, as the prescriptive requirements often
133 become an obstacle for implementing more environmentally friendly solutions.

134

135 In the present project, the reference concrete (starting point for development of concrete mixtures)
136 was a concrete mixture from a ready mix plant that fulfilled all the above-mentioned prescriptive
137 requirements:

138

- 139 • Cement type: CEM I 42.5 N – SR5 (alkali content < 0.4%)
- 140 • $FA/(C+FA) = 0.13$
- 141 • $W/C_{eq} = 0.37$

142

143 The aim was to obtain comparable technical performance with regard to workability, compressive
144 strength, and salt frost scaling resistance (see section 2.3 for exact requirements). The carbon
145 footprint of the cement used in the reference concrete was relatively high. Therefore, it was decided
146 to use another type of cement (CEM I 52.5 N) with a lower carbon footprint. Because of the higher
147 strength potential of the cement, the W/C_{eq} was increased to obtain the same compressive strength
148 as the reference concrete. Therefore, none of the mixtures in the present study met the Danish rules
149 as regards maximum W/C_{eq} .

150

151 **2.2 Materials**

152 The cement used in the study was type CEM I 52.5 N according to EN 197-1 [16]. The fly ash used
153 was low in calcium oxide (CaO) and conformed to EN 450-1 [17]. The chemical compositions of
154 cement and fly ash are shown in table 1. Chemical analyses have not been performed as part of this

155 project, so chemical compositions are according to information from the manufacturers. For the fly
156 ash, it is an average for 6 months of production.

157

158 *Table 1: Chemical composition of powders. Figures are in unit [% of powder mass].*

	CaO	SiO ₂	Al ₂ O ₃	Fe ₂ O ₃	SO ₃	Na ₂ O eq	Cl ⁻	LOI
Cement	64.5	19.7	5.2	3.8	3.3	0.6	≤ 0.05	1.7
Fly ash	3.9	56.4	21.6	5.4	0.6	2.9	≤ 0.05	2.1

159

160 Tap water was used as mixing water.

161

162 The coarse aggregates were 3 size fractions of crushed granite. They were all suitable for aggressive
163 environment (frost and chloride exposure, exposure classes XF4 according to EN 206 [15]).

164

165 Two chemical additives were used:

- 166 • superplasticizer, active component: polycarboxylates
- 167 • air entraining agent, active component: tensides

168

169 **2.3 Concrete specimens**

170 Concrete compositions for mixtures with various contents of fly ash were developed in a 3 step
171 process. The process followed the same procedure as the Danish development project “Green
172 Transition of Cement and Concrete Production” (mentioned in section 1), where concrete mixtures
173 with high contents of fly ash had failed accelerated salt frost scaling testing.

174

175 First, a desktop calculation was made, based on a performance-based design procedure developed in
176 the project “Green Transition of Cement and Concrete Production”. The design procedure is
177 described in [18]. The procedure is based on interpolation between results obtained for concrete
178 mixtures with varying fly ash contents. The design procedure ensures that the concrete mixture with
179 the highest cement substitution that fulfills the technical requirements will be chosen, thereby
180 leading to a concrete composition with minimum carbon footprint. Concrete compositions were
181 developed with FA/(C+FA) 0%, 25%, 33%, 44%, and 50%, aiming at the same workability, air
182 content, and compressive strength for all mixtures:

183

- 184 • Slump: 125 mm
- 185 • Air content in fresh concrete: 6%
- 186 • Compressive strength after 28 days of curing at 20°C: 42 MPa

187

188 The aggregate content and combination was identical in all mixtures, i.e. changes only concerned
189 the composition of the paste. Mixtures were identified by their FA/(C+FA) ratio. For example,
190 mixture 033 is the mixture with $FA/(C+FA) = 33\%$.

191

192 Second, trial mixing was performed for all concrete compositions. Trial mixing was performed by
193 mixing 9 l concrete in a small laboratory pan mixer. Here, the slump and air content of the fresh
194 concrete were measured. The following acceptance criteria were used:

195

- 196 • Slump: 125 ± 25 mm
- 197 • Air content in fresh concrete: $6.0 \pm 1.0\%$

198

199 If the fresh concrete properties did not match the acceptance criteria, the dosages of superplasticizer
200 and air entraining agent were adjusted, until the fresh concrete properties were satisfactory. From
201 the last trial mix of all concrete compositions, specimens were cast for measurements of
202 compressive strength, before the compositions were finally approved.

203

204 The final concrete compositions are shown in table 2. When reviewing the compositions for
205 mixtures 000-050, it was noticed that the dosage of superplasticizer increased, when the content of
206 fly ash increased. It was expected that the dosage of air entraining agent would also unequivocally
207 increase, when the fly ash content increased. However, the figures showed that the amount of air
208 entraining agent reached a maximum at $FA/(C+FA) = 0.25$. Superplasticizers sometimes also
209 possess air entraining abilities, and then to keep a constant total air content, it is necessary to reduce
210 the dosage of air entraining agent. However, air voids generated by a superplasticizer typically are
211 coarser than air voids generated by an air entraining agent [7]. It was therefore decided to add an
212 extra mixture to the experimental program. This mixture should represent the combination of a high
213 $FA/(C+FA)$ and a high dosage of air entraining agent. This mixture was called 050EA (EA: Extra
214 Air entraining admixture). 050EA was identical to mixture 050, except for the AEA dosage, which
215 was identical to mixture 025 that had the highest dosage of AEA of all the other mixtures. This
216 dosage also corresponded to the maximum recommended dosage according to the technical data
217 sheet from the AEA manufacturer. During the trial mixing of mixture 050EA, the dosage of AEA
218 was not adjusted to meet target values of fresh concrete properties. A small adjustment was made
219 for the dosage of superplasticizer to meet the target slump. The mixture was approved after it was
220 ensured that the mixture did not show signs of separation or other aspects that could cause casting
221 difficulties. Compressive strength was not used as acceptance criterion for mixture 050EA, as it was
222 expected that the high air content registered in the fresh concrete would lead to a strength reduction.

223

224 *Table 2: Concrete compositions (expected air content in fresh concrete: 6%). Aggregates are in*
 225 *saturated, surface dry condition.*

Constituents	Density	Mixture					
		000	025	033	044	050	050EA
	[kg/m ³]	[kg/m ³]	[kg/m ³]	[kg/m ³]	[kg/m ³]	[kg/m ³]	[kg/m ³]
Cement	3160	372	291	267	234	218	218
Fly ash	2300	-	96	133	188	218	218
Water	1000	181	170	156	144	135	131
Sand, 0-4 mm	2620	620					
Coarse agg., 5-8 mm	2700	173					
Coarse agg., 8-16 mm	2720	370					
Coarse agg., 16-25 mm	2720	544					
Superplasticizer	1050	0.2	0.4	0.8	1.9	2.6	2.8
Air entraining agent	1010	4.5	7.0	5.0	2.5	2.7	7.0

226

227 Third, all mixtures were prepared in a pan mixer of semi-industrial size (batch size 175 l). Previous
 228 experience had shown good reproducibility between results obtained using the laboratory mixer
 229 used for trial mixing and the larger mixer. For each mixture, slump and air content in fresh concrete
 230 were measured according to Euro norms [19, 20]. If the measurements corresponded to expected
 231 values (i.e. values from the trial casting) within reasonable accuracy, the mixture was used to cast
 232 18 Ø150 x 300 mm cylinders. The specimens were de-moulded 24 h after casting. The subsequent
 233 curing of the test specimens depended on the test method that the specimens were going to be used
 234 for, i.e. testing of compressive strength (section 2.5), air void analysis (section 2.6) and accelerated
 235 salt frost scaling testing (section 2.7).

236

237 **2.4 Paste specimens**

238 Paste samples were produced to investigate how the presence of fly ash cenospheres can influence
239 the outcome of air void analysis of hardened concrete. Each paste mixture corresponded to a
240 concrete mixture, see table 2. The paste was produced using cement, possibly fly ash, and water.
241 The paste was prepared without superplasticizer and air entraining agent, so the paste was not in
242 any way air entrained. It was assumed that air voids registered during the air void analysis would
243 mainly be due to cenospheres.

244

245 0.4 l paste was produced for each mixture. The paste was mixed manually. The mixing water was
246 gradually added to the powder to ensure a homogenous paste without lumps. When all water had
247 been added, the paste was mixed for 3 minutes. The paste was cast in Ø22 x 120 mm cylindrical
248 tubes (1 tube per mixture). The paste was cautiously placed in the tubes to prevent entrapped air.
249 During the first 24 hours of hardening, the tubes were rotated to prevent separation. After 24 hours,
250 the tubes were de-moulded and the paste specimens were sealed and stored in a climate room
251 (20°C) until time of air void analysis.

252

253 **2.5 Compressive strength**

254 The compressive strength was measured according to EN 12390-3 [21]. The test was carried out for
255 3 specimens from each mixture. After de-moulding, the specimens were placed in a 20°C water
256 bath, and the test was carried out, when the test specimens were 28 days old. It was decided to
257 strictly follow the standardized test, including the before-mentioned curing regime, even though this
258 meant that the curing conditions for specimens for compressive strength testing and for accelerated
259 salt frost scaling testing were not alike, see section 2.7.

260

261 **2.6 Air void analysis of hardened paste and concrete samples**

262 The air void analyses were carried out according to EN 480-11 [22], using the RapidAir image
263 analysis system for measurements of the air void parameters.

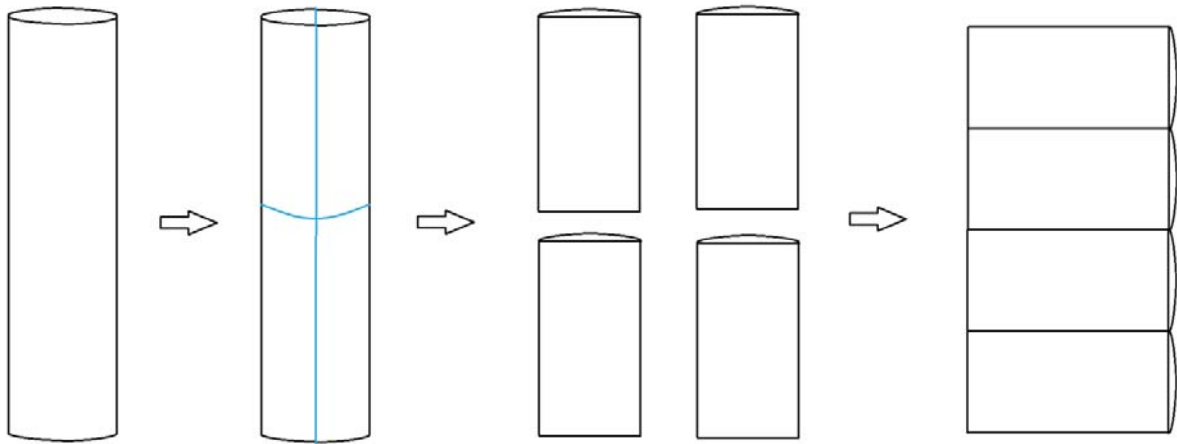
264

265 Air void analyses were carried out for 2 concrete cylinders for each mixture (total traverse length:
266 1200 mm per specimen). After de-moulding, the cylinders were stored in water (20°C) until the
267 time of testing. All concrete specimens were at least 14 days old at time of testing. The air void
268 structure does not change in the hardened concrete. Therefore, time of testing is not critical, as long
269 as the concrete strength is adequate to ensure good sample preparation.

270

271 The air void analysis was carried out for one paste cylinder for each mixture (at least 14 days at
272 time of testing). The specimen was saw cut both crosswise and lengthwise and then glued together,
273 see figure 2. This was done to obtain a test area that at the same time was as large as possible, and
274 almost quadratic, as this eased the grinding. By doing so, the test area became approx. 60 mm x 95
275 mm. The total traverse length for each specimen was 600 mm. This was only half of the required
276 traverse length according to [22]. However, the purpose of this standard is to analyze concrete and
277 mortar, not paste. For concrete samples, aggregates normally constitute more than 50% of the test
278 area, and the traverse length in paste is therefore less than 600 mm. Thus, the traverse length for the
279 paste samples in the present study was longer than the traverse length in paste for concrete samples.
280 For this reason, it was considered acceptable to reduce the traverse length to 600 mm.

281



282

283 *Figure 2: Cutting and gluing of paste specimens for air void analysis.*

284

285 **2.7 Accelerated salt frost scaling test**

286 Accelerated salt frost scaling tests were carried out according to the reference method in CEN/TS
 287 12390-9 [23]. After de-moulding, concrete cylinders were stored 6 days in water (20°C), and then
 288 stored in climate chamber (20°C, 65% RH) until the age of 28 days. During the period in climate
 289 chamber, the specimens were only removed for short periods of time to saw cut the specimens (day
 290 21) and to glue on a rubber sleeve (day 25). The rubber sleeve made it possible to establish a liquid
 291 reservoir on top of the specimen. At the age of 28 days, the test surface was covered with 3 mm of
 292 de-ionised water to obtain capillary saturation in the surface layer. The specimen was covered with
 293 a plastic sheet to prevent evaporation. At the age of 31 days, the de-ionised water was replaced with
 294 a 3% NaCl solution, and the freeze-thaw exposure was initiated by placing the specimens in a
 295 freezing chamber. The freezing chamber was controlled by a thermocouple placed in the liquid
 296 layer on one of the test specimens. The temperature in the liquid layer followed a temperature cycle
 297 defined in the standard. During the temperature cycle, the temperature started at +20°C and was
 298 then gradually decreased to -20°C, before the temperature was again increased to +20°C. Each

299 temperature cycle lasted 24 h, and the samples were exposed to a total of 56 cycles. Scaled material
300 from the samples were collected after 7, 14, 28, 42, and 56 cycles.

301

302 **3. Results and discussion**

303

304 **3.1 Results from concrete samples**

305 The results from testing performed on the concrete specimens are shown in table 3. Where nothing
306 else is mentioned, the results are for concrete from the final mixtures. However, as regards
307 compressive strength, results are shown both for concrete from the trial mixtures and the final
308 mixtures (concrete compositions are identical).

309

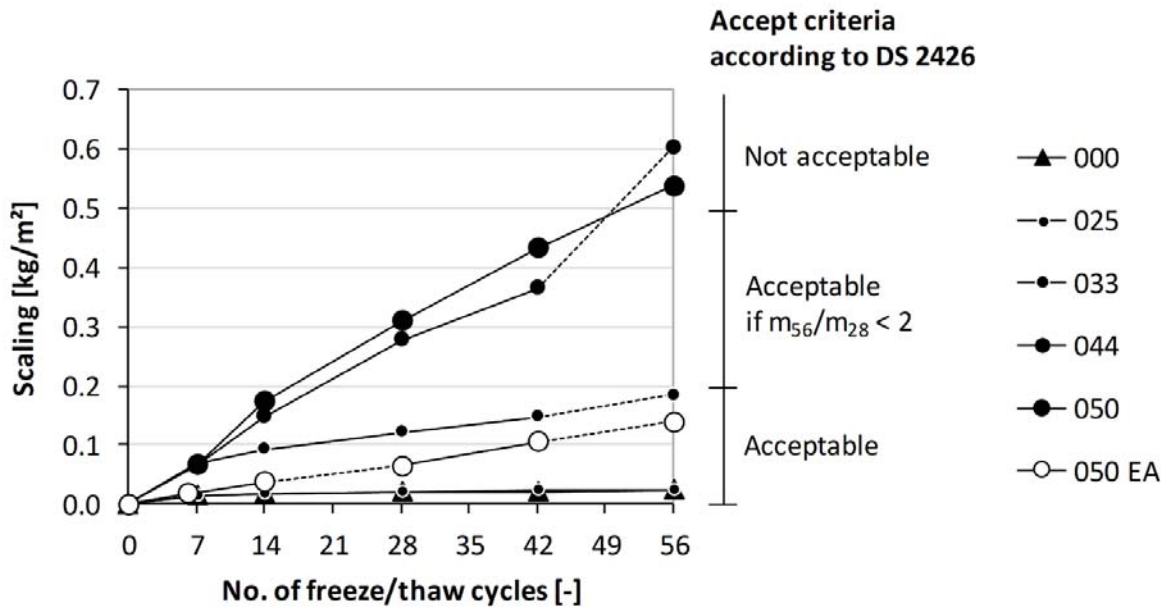
310 *Table 3: Results from tests performed on fresh and hardened concrete.*

Mixture ID	Slump	Air content in fresh concrete	Air content in hardened concrete	Specific surface	Spacing factor	Compressive strength trial mix	Compressive strength final mix	Accumulated scaling after 28 cycles	Accumulated scaling after 56 cycles
	[mm]	A _{fresh} [%]	A _{hard} [%]	S [mm ⁻¹]	L [mm]	[MPa]	[MPa]	m ₂₈ [kg]	m ₂₈ [kg]
000	110	6.4	7.33	42.2	0.081	42.9	44.1	0.02	0.02
025	110	7.0	6.44	47.1	0.080	39.2	38.8	0.02	0.03
033	110	5.6	5.03	40.8	0.118	-(1)	46.2	0.12	0.19
044	125	5.8	4.31	44.2	0.112	41.7	59.5	0.28	0.60
050	125	5.5	4.74	40.4	0.119	44.4	61.3	0.31	0.54
050EA	100	8.5	7.57	44.3	0.075	-(2)	40.9	0.07	0.14

- 311 1. The compressive strength for mixture 033 was not measured for specimens from the trial casting
312 (unintentional omission).
313 2. The compressive strength for mixture 050EA was not measured during trial casting. Due to the
314 increased dosage of air entraining agent compared to mixture 050, mixture 050EA was expected
315 to have lower strength than mixture 000, and therefore equal strength was not an accept criterion
316 for mixture 050EA during trial casting.
317

318 The development in salt frost scaling is shown in figure 3. Unfortunately, the freezing chamber
319 broke down twice during the test period. This happened during a weekend and during a public
320 holiday, so each time the problem was unfortunately not discovered before several days later.
321 During the break downs, the freezing chamber did not start a new freeze/thaw cycle, and the
322 specimens were stored at approx. 25°C. When the problem was discovered, the freezing chamber
323 was restarted, and the test period was prolonged, so all specimens experienced 56 freeze/thaw
324 cycles. As the mixtures had not been cast on the same day, the specimens did not have the same
325 age, when the problem with the freezing chamber occurred. The dashed line between two markers
326 indicate for each mixture when the problem occurred.

327



328

329 *Figure 3: Development of freeze/thaw scaling in the experiment together with acceptance criteria*
330 *for cumulated scaling after 56 freeze/thaw cycles according to DS 2426 [14] (DS 2426 allows more*
331 *scaling, if the development of scaling is not accelerating, i.e. $m_{56}/m_{28} < 2$).*

332

333 Based on results shown in table 4 and in figure 3, the following is observed:

334

- 335 • The properties of the fresh concrete, i.e. slump and air content, are as expected.
- 336 • If not taking mixture 050EA into account, there seems to be a trend, where the total air content
337 in the hardened concrete is reduced, when the fly ash content is increased. This may be because
338 the dosage of AEA is low in the mixtures with high contents of fly ash, i.e. the dosage of AEA
339 is lower in mixture 044 and 050 than in mixture 000, and this may cause the air voids to be less
340 stable in mixtures with high fly ash contents.

- 341 • Even though the total air content of mixtures with high volumes of fly ash are reduced, they still
342 show low spacing factors. The largest spacing factor is registered for mixture 050, and here the
343 value is 0.119 mm. This is well below 0.20 mm, which is often considered the critical spacing
344 factor [24].
- 345 • For the trial mixtures, the 28 days compressive strength is on the same level for all mixtures
346 (39.2-44.4 MPa).
- 347 • For the final mixtures, mixtures 000, 025, and 033 show compressive strength on the same level
348 as the trial mixtures. For mixtures 044 and 050, the compressive strengths are much higher than
349 for the corresponding trial mixtures; the compressive strength of mixtures 044 and 050 are 59.5
350 MPa and 61.3 MPa, respectively, compared to 44.1 MPa for mixture 000. The reason why the
351 compressive strengths of mixtures 044 and 050 are higher is not known. The compressive
352 strength of mixture 050EA is 8% lower than for mixture 000. This may be due to the high total
353 air content of mixture 050EA; it shows the highest air content of all mixtures, both in the fresh
354 and in the hardened concrete.
- 355 • None of the mixtures showed accelerating scaling during the 56 freeze/thaw cycles, i.e. in all
356 cases the cumulated scaling after 56 cycles m_{56} is less than twice the amount of cumulated
357 scaling after 28 cycles m_{28} ($m_{56}/m_{28} < 2$). DS 2426 sets up different acceptance criteria
358 depending on if the scaling is accelerating or not. In the present case, where the development of
359 scaling is not accelerating, up to 0.50 kg/m² scaling after 56 freeze/thaw cycles is acceptable.
- 360 • The frost resistance of mixtures 044 and 050 were not acceptable, even though they showed
361 high compressive strength and acceptable air void structures.
- 362 • Mixture 050EA showed acceptable frost resistance. However, even though mixture 050EA both
363 had the highest total air content and the lowest spacing factor of all mixtures, the frost resistance
364 of mixture 050EA was not as good as the frost resistance of mixtures 000 and 025.

365

366 3.2 Results from paste samples

367 Table 4 shows the results from the air void analysis of paste samples:

368

369 *Table 4: Air void analysis of hardened paste samples.*

Mixture ID	Air content in hardened paste	Specific surface	Spacing factor
	A_{hard} [%]	S [mm^{-1}]	L [mm]
000	0.75	30.3	0.611
025	1.75	63.0	0.212
033	1.26	88.6	0.171
044	2.63	57.2	0.197
050	2.10	98.4	0.125

370

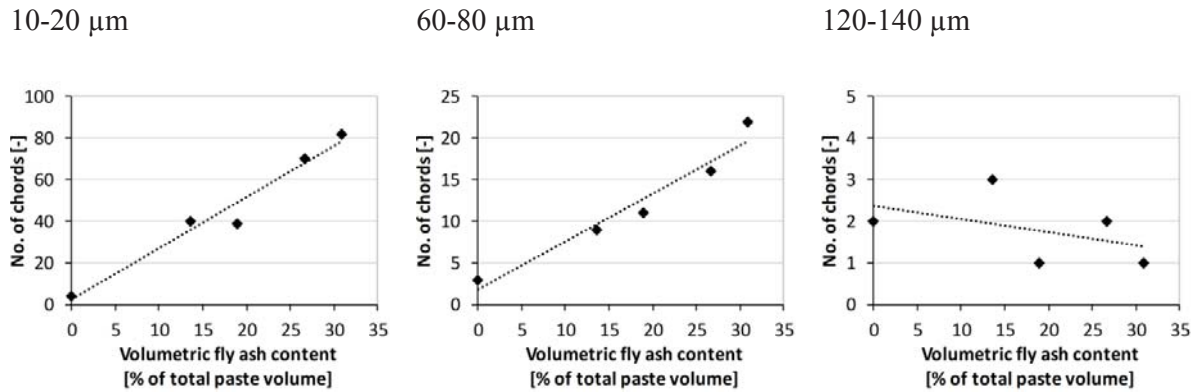
371 The general trend is that the total air content as well as the specific surface of air voids registered in
372 the hardened paste sample increase, when the fly ash content increases. As a consequence, the
373 spacing factor decreases, when the fly ash content increases. None of the samples are air entrained,
374 so they should show spacing factors considerably higher than the critical spacing factor of 0.20 mm.
375 This is also the case for the reference mixture (mixture 000), but the mixtures with the highest fly
376 ash contents, i.e. mixtures 033, 044, and 050, all show spacing factors lower than 0.20 mm.

377

378 In the paste mixtures 000, 025, 033, 044, and 050, the fly ash makes up 0%, 14%, 19%, 27%, and
379 32% of the paste volume. If the cenospheres show up as air voids in the air void analysis, then the
380 number of chords in each size interval is proportional to the fly ash volume. Therefore, the number

381 of chords in each of the 28 chord size intervals according to EN 480-11 is plotted as a function of
382 volumetric fly ash content. Figure 4 shows the plots for 3 different chord size intervals:

383



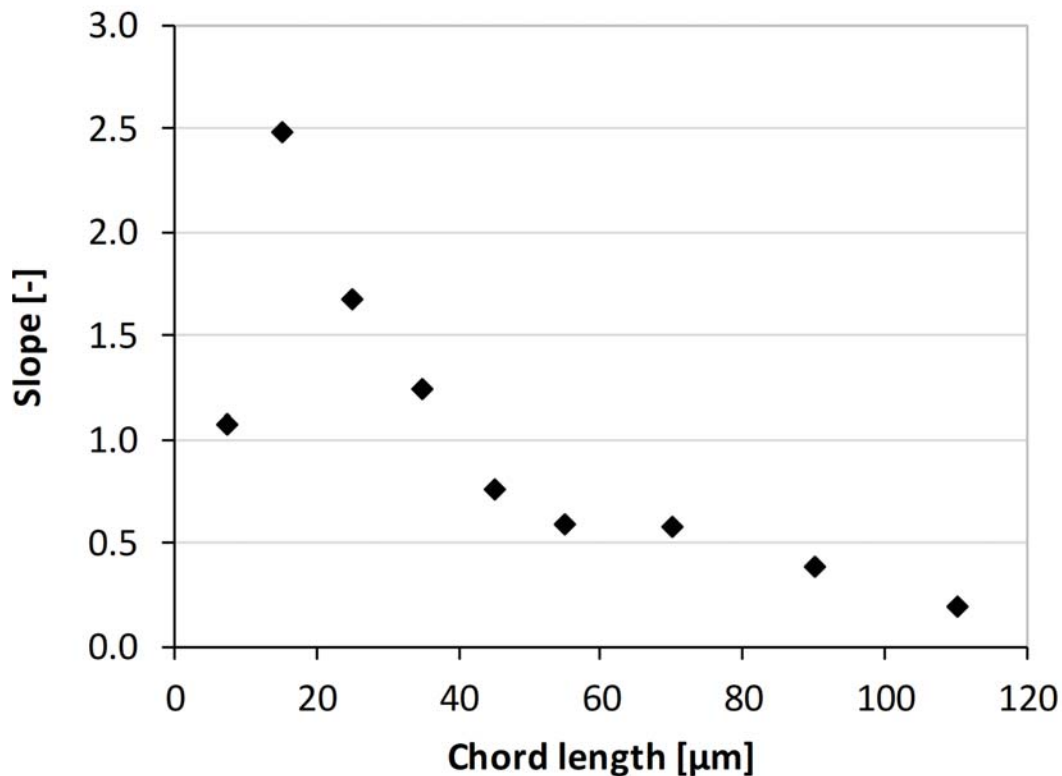
384 *Figure 4: Number of chords versus volumetric fly ash content, plotted for 3 different chord size*
385 *intervals (Note: Scaling of vertical axes are different).*

386

387 Up to chord size interval 100-120 μm, there is a linear relation between the number of registered
388 chords in the size interval and the fly ash volume. When there is no fly ash in the cement paste,
389 nearly no chords are registered, and then the number of chords increases, when the fly ash volume
390 increases. From chord size 120-140 μm and up, the number of registered chords are in all cases low,
391 and their number seems to be at random with no relation to fly ash content. This supports the
392 hypothesis that the presence of cenospheres distort the outcome of the air void analysis. At small
393 chord sizes, many of the registered voids are not air voids but cenospheres. For the majority of the
394 fly ash particles, the diameter is less than 100 μm, and therefore the cenospheres do not add to the
395 registered number of chords at larger chord sizes. Here, it is entrapped air that is registered. Even
396 though the paste samples were carefully compacted, the entrapped air could not be completely
397 avoided, but the amount of entrapped air does not seem to be correlated to the fly ash content.

398

399 From the slope of the trend line in each graph up to chord size 100-120 μm , it is possible to
400 calculate how much the presence of cenospheres contribute to the air void analysis, see figure 5:
401



402 *Figure 5: The contribution of cenospheres to the air void analysis. The slope has been determined*
403 *for separate graphs like those shown in figure 4. The slope corresponds to the number of chords per*
404 *600 mm traverse length, when the volumetric fly ash content is 1% of the paste volume.*

405

406 Figure 5 shows that except for the smallest chord size interval (0-10 μm), the graph is a gradually
407 decreasing line. The reason for the low number of chords in the size interval 0-10 μm is that the
408 RapidAir image analysis system sorts out all chords shorter than 6 μm , as they are considered noise.

409

410 **3.3 Combining results from concrete and paste experiments**

411 The results shown in figure 5 can be used to correct the air void analyses that were performed for
412 the concrete samples. For each mixture, steps 1-4 are performed:

413

414 1. Calculate the volumetric fly ash content

415 2. Given the volumetric fly ash content and the linear traverse length in the original air void
416 analysis, calculate the expected number of chords generated due to cenospheres in each chord
417 size interval.

418 3. Subtract the expected number of chords due to cenospheres from the number of chords in each
419 chord size interval registered in the original air void analysis. The result is a corrected chord
420 table.

421 4. Use the corrected chord table to calculate the total air content and specific surface area of air
422 voids; these figures can then be used to calculate the spacing factor.

423

424 Table 5 shows results from the original and the corrected air void analyses, respectively:

425

426 *Table 5: Results from the original air void analysis and results after the chord table has been*
 427 *corrected to take the presence of voids generated by cenospheres into account.*

Mixture ID	Air content in hardened concrete		Specific surface		Spacing factor	
	A_{hard} [%]		S [mm ⁻¹]		L [mm]	
	original	corrected	original	corrected	original	corrected
000	7.33	-	42.2	-	0.081	-
025	6.44	6.32	47.1	44.9	0.080	0.091
033	5.03	4.86	40.8	36.6	0.118	0.135
044	4.31	3.99	44.2	37.6	0.112	0.137
050	4.74	4.34	40.4	33.2	0.119	0.152
050EA	7.57	7.18	44.3	40.2	0.075	0.087

428

429 For all air void parameters, the largest correction is made for mixture 050. With regard to total air
 430 content, the correction for mixture 050 is 0.40% (percentage point). This is also the largest
 431 correction relative to the total air content before the correction (8%). The correction of specific
 432 surface is more distinct. For mixture 050, the specific surface is reduced 18% due to the correction.
 433 Both the correction of the total air content and the correction of the specific surface has an impact
 434 on the calculated spacing factor. All the corrected spacing factors are still below the critical spacing
 435 factor of 0.20 mm. However, the difference between a spacing factor of 0.081 mm (mixture 000)
 436 and a spacing factor of 0.152 mm (mixture 050) is significant, and they cannot be said to be on the
 437 same level within the accuracy of the method.

438

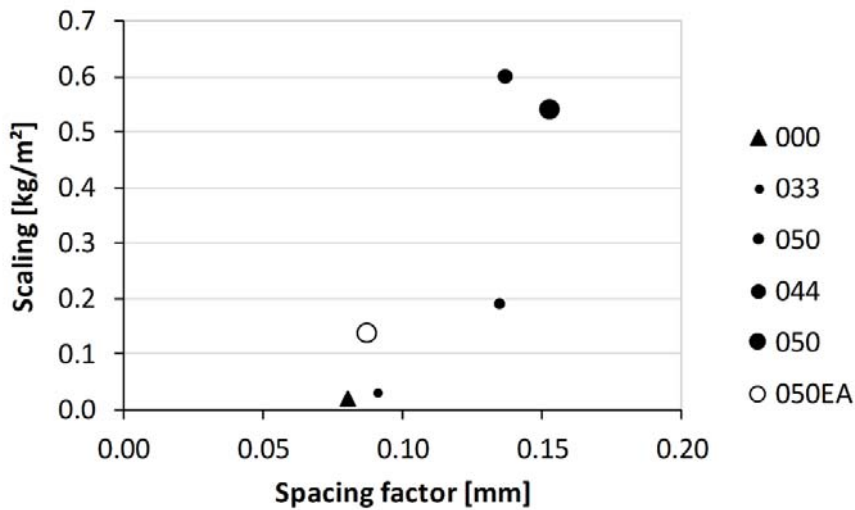
439 The effect of cenospheres on the outcome of air void analysis has to the knowledge of the authors
 440 not been quantified before. The results from the present study are not directly transferrable to other

441 studies with high contents of fly ash, where air void analyses have been performed, as the amount
442 of cenospheres in the fly ash and the size distribution of voids generated by the cenospheres are
443 closely related to the fly ash source. However, it is reasonable to assume that also in other studies
444 reported in the scientific literature, the air void analyses may misrepresent the actual air void
445 structure if the concrete contains a high volume of fly ash. For example in [25], where Yildirim et
446 al. test FA/C ratios that are even higher than in the present study. In their study, mortars with FA/C
447 ratios 1.2, 2.2, and 4.2 are tested This corresponds to FA/(C+FA) ratios 0.55, 0.69, and 0.81. Even
448 though the mixtures are not air entrained, they show spacing factors of 0.129 mm, 0.069 mm, and
449 0.057 mm, respectively. Likewise, there seems to be a systematic trend, where higher fly ash
450 contents result in lower spacing factors. The water to cementitious material (W/CM) ratio is in all
451 cases 0.27. Despite the low W/CM ratio and the seemingly good air void structure, none of the
452 mixtures passes an accelerated freeze/thaw test.

453

454 Figure 6 shows the cumulated scaling after 56 freeze/thaw cycles (also depicted in figure 3), but
455 here as a function of the corrected spacing factor:

456



457

458 *Figure 6: Cumulated scaling after 56 freeze/thaw cycles vs. corrected spacing factor.*

459

460 Figure 6 shows that although the corrected spacing factor of mixture 050EA is on the same level as
 461 the spacing factors of mixtures 000 and 025, the scaling due to frost action is approximately 5 times
 462 higher. Figure 6 also shows that for mixtures 044 and 050, the scaling is considered critical, even
 463 though the spacing factors are lower than 0.20 mm, which is normally an acceptable spacing factor.
 464 It is therefore concluded that the presence of cenospheres only partly can explain why the frost
 465 resistance of concrete with high contents of fly ash performed worse in accelerated freeze/thaw tests
 466 than anticipated based on information on the concrete composition and results from air void
 467 analysis; the presence of cenospheres is not likely to be the full explanation.

468

469 Valenza and Scherer state that the inferior salt frost scaling resistance of concrete with high
 470 contents of fly ash may be caused by the curing procedure used prior to freeze/thaw testing [26]. In
 471 the present study a standardized method is used, where the concrete is sealed the first day after
 472 casting, then it is submerged in water for 6 days and finally stored 21 days at 20°C, 65% RH. This
 473 procedure may be representative for e.g. an in-situ casting, as drying protection normally is not

474 maintained for more than a week. However, it is likely that a short moist curing period will lead to a
475 larger strength reduction for concrete with fly ash, compared to concrete with cement as the only
476 binder, because concrete with a high content of fly ash due to slower hydration is more vulnerable
477 to loss of water. The lower strength will again result in inferior salt frost scaling resistance. It may
478 be speculated that the compressive strength measured in the present study is not identical to the
479 strength of the specimens that were subjected to accelerated freeze/thaw testing, because the curing
480 procedures of the two standardized test methods were not alike (see sections 2.5 and 2.7). Data from
481 literature may indicate the magnitude of the difference. Ramezaniapour and Malhotra measured
482 compressive strength development for concrete cured at various conditions [27]. For concrete with
483 cement as only binder, the 28 days compressive strength of concrete moist cured 2 days after
484 demoulding and then left in the laboratory (23°C, RH not specified) was 95% of the compressive
485 strength of concrete that had been moist cured all the time between demoulding and testing. For
486 concrete where low calcium fly ash constituted 58% of the binder, the compressive strength for
487 concrete moist cured 2 days after demoulding was only 86% of the strength registered for concrete
488 that was fully moist cured. In another study [28] with similar binder compositions (57% low
489 calcium fly ash in concrete with high contents of fly ash), cast concrete cylinders were either stored
490 in a fog room (23°C, RH>95%) until time of testing, or they were stored 7 days under wet burlap in
491 the laboratory and then air-cured outdoor. Here, the 28 days compressive strength of concrete
492 specimens cured in air is approximately 80% of the strength for moist-cured specimens. However, it
493 also has to be taken into account that the outdoor temperature was lower than the temperature in the
494 fog room. In a recent review [29], results are compared for concrete with fly ash, where the
495 specimens are either moist cured (20°C, in water bath or in fog room) or moist cured for 7 days and
496 then air dried (20°C, 65% RH). The review comprises more than 100 concrete mixtures with low
497 calcium fly ash (up to 50% of the binder content) for each drying condition. The conclusion is that

498 there is no systematic difference between the two curing conditions. The difference in curing
499 conditions in [29] is similar to the difference in curing conditions for specimens for compressive
500 strength testing and accelerated freeze/thaw testing, respectively in the present study. If strength
501 reduction due to drying should explain the poor salt frost scaling resistance for mixtures 044 and
502 050, then the strength reduction should be approximately 30% to match the strength of mixture 000.
503 A 30% strength loss does not seem plausible, when the strength reduction is only up to 20% in [27,
504 28], where the drying condition during air curing is more severe.

505

506 The results of the present study indicates that neither the presence of cenospheres nor strength
507 reduction due to drying can explain the susceptibility to salt frost scaling. Therefore, there seems to
508 be at least one other reason why concrete with high contents of fly ash is vulnerable to salt frost
509 scaling.

510

511 **4. New hypothesis: Combined action of several degradation mechanisms**

512 It was decided to conduct a follow-up investigation comprising fluorescent epoxy impregnated thin
513 section analysis and scanning electron microscopy (SEM) of the freeze/thaw exposed test surfaces.
514 Figure 7 shows selected photos of thin sections. Figure 8 shows an example of a SEM photo.

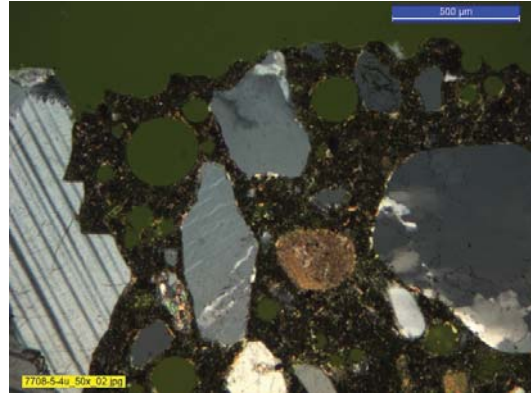
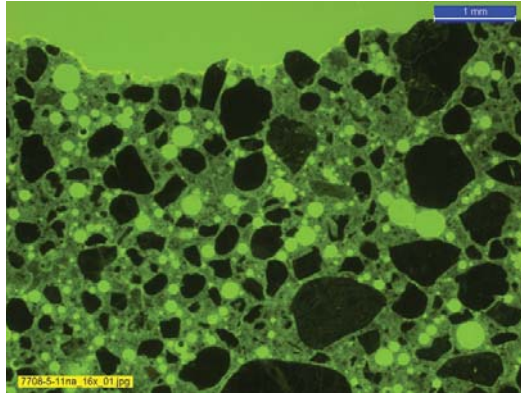
515

Mixture ID

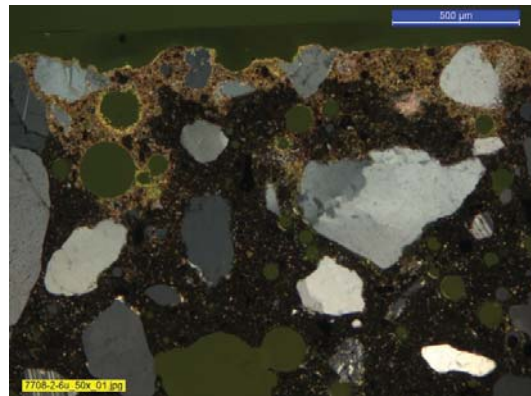
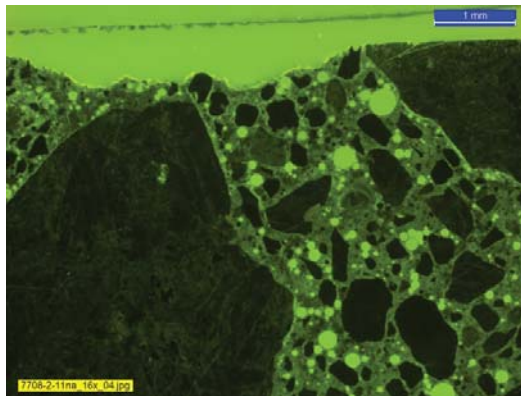
Microscope setting:
Fluorescence light mode
(magnification: blue bar equals 1 mm)

Microscope setting:
Cross polarized light mode
(magnification: blue bar equals 0.5 mm)

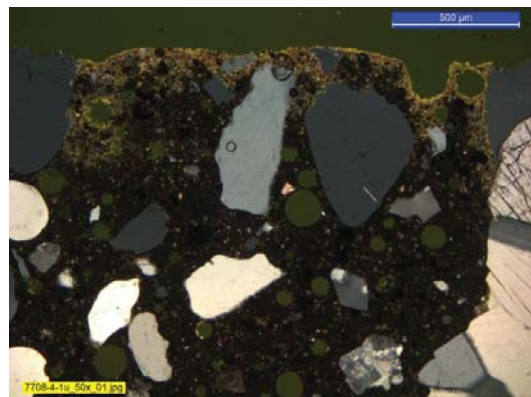
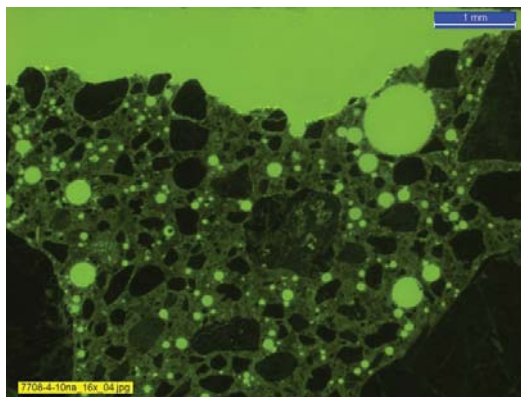
000



033

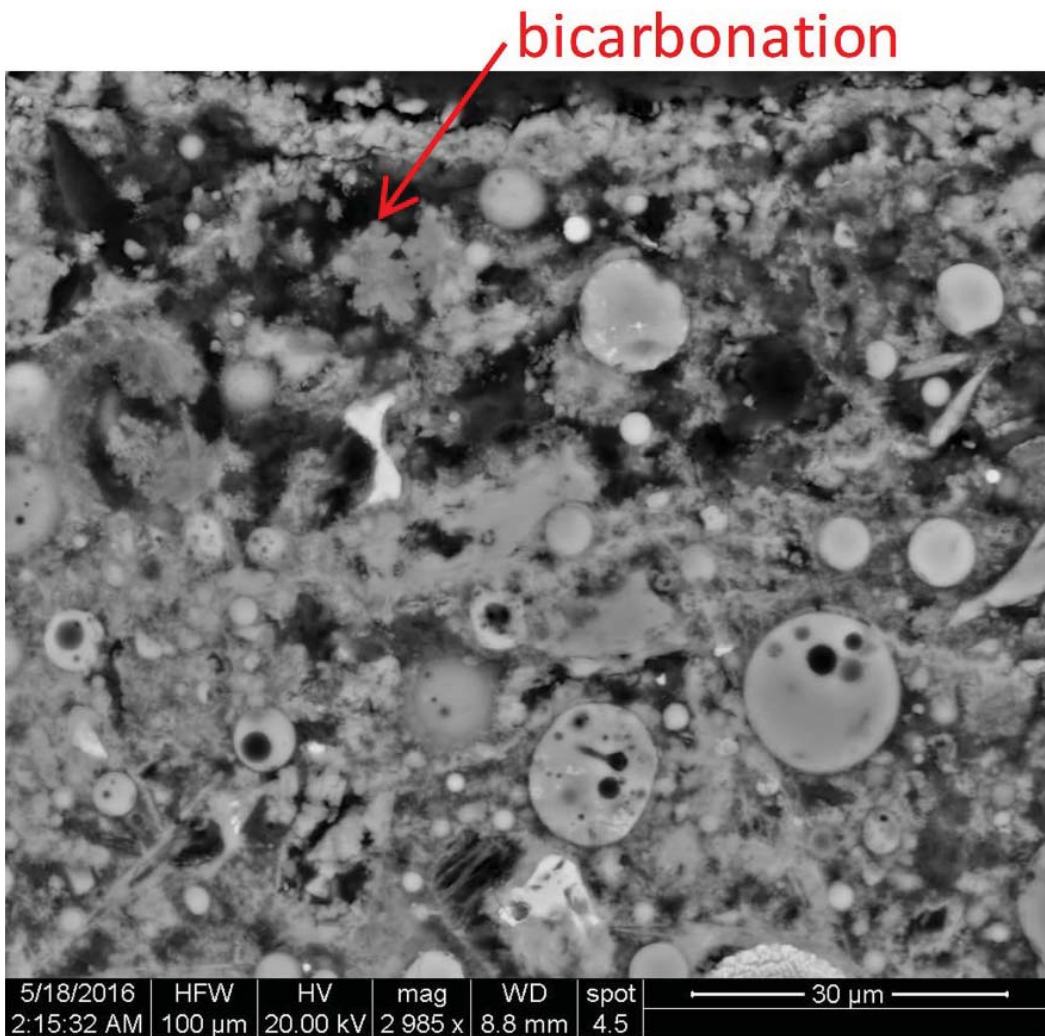


050



516 *Figure 7: Concrete surfaces after exposure to freezing and thawing.*

517



518 *Figure 8: SEM photo of specimen from mixture 033 after freeze/thaw exposure (magnification: blue*
 519 *bar equals 30 micrometers).*

520

521 The following observations are made during the examination of the surfaces:

522

- 523 • The thin sections show that all concrete mixtures have systems of fine and well-dispersed air
- 524 voids as also shown by the air void analyses.

- 525 • After freeze/thaw exposure, the surface roughness increases for specimens that have shown
526 scaling. However, the specimens that have suffered from scaling do not show signs of inner
527 cracking.
- 528 • All specimens except the specimen from mixture 000 show a carbonated zone just below the
529 test surface after freeze/thaw exposure. The thickness of the carbonated layer is highest for
530 mixtures 025 and 033, where the extent of the carbonated zone is approximately on the same
531 level.
- 532 • SEM photos show bicarbonation (“popcorn calcite”) in the carbonated layer for all samples
533 except mixture 000.

534

535 Several things seem unusual. For example, no signs of inner cracking are seen in the concrete that at
536 the same time shows severe scaling during the salt frost scaling test. For concrete in general, there
537 will normally be fine cracks in the zone just below the scaled surface [30]. However, our
538 observation of salt frost scaling without inner cracking is not without precedent for concrete with
539 high contents of fly ash. Bilodeau et al [31] made a study comprising 2 types of cement and 8
540 different types of fly ash (16 mixture combinations). In all mixtures, fly ash made up 63% of the
541 powder by mass, $W/(C+FA)=0.33$, and all mixtures were air entrained (spacing factors in the range
542 0.11-0.21 mm). All mixtures were tested both according to ASTM C 666 procedure A (freezing and
543 thawing in pure water) and according to ASTM C 672 (salt frost scaling test). In the ASTM C 666
544 test, 13 of 16 mixtures showed durability factors surpassing 100 after 1000 freeze/thaw cycles, and
545 all mixtures passed the test. Thus, there was no indication of the high volume fly ash mixtures
546 having problems with inner cracking. However, all mixtures showed levels of salt frost scaling
547 during the ASTM C 672 test that were not satisfactory; all mixtures except one received the visual

548 rating 5 (severe scaling) already after 50 freeze/thaw cycles, and the last mixture was rated 4
549 (moderate to severe scaling).

550

551 In the present study, it is also surprising that carbonation has developed in the surface layer of most
552 specimens during freeze/thaw exposure. During testing, the specimens were covered by 3 mm of
553 NaCl solution, and the solution was again covered with a plastic sheet to prevent evaporation, so the
554 exposure to CO₂ from atmospheric air in the freezing chamber was very limited. The freeze/thaw
555 test was performed for 3 specimens for each mixture. Originally, 4 specimens were prepared for
556 testing, but the fourth specimen was never placed in the freezing chamber. Therefore, it was
557 possible to make thin sections from these extra specimens, which had followed the test scheme until
558 31 days after casting, including 3 days of capillary suction with de-ionised water. These thin
559 sections did not show signs of carbonation, confirming that the carbonation had taken place during
560 the period of freeze/thaw exposure.

561

562 Even though the highest carbonation depth is observed for mixtures 025 and 033, it is not evident
563 that carbonation happens faster for these mixtures than for mixtures 044 and 050, as carbonation
564 depth is measured relative to the surface after scaling has been removed. In fact, it could well be
565 that carbonation has progressed further in mixtures 044 and 050 than in mixtures 025 and 033, but
566 for mixtures 044 and 050 part of the carbonated layer has been removed due to scaling.

567

568 It is therefore suggested that for concrete mixtures with high contents of fly ash, surface scaling is
569 due to combined action of chemical degradation and frost action. Bicarbonation appears in concrete
570 with a low content of calcium hydroxide [31]. Where regular carbonation may lead to a
571 densification of the concrete and thereby slow down transport of matter in the surface layer [33],

572 bicarbonation reduces concrete strength and makes the concrete more permeable [31]. If a chemical
573 reaction takes place in the surface layer and thereby locally reduces the concrete quality, the surface
574 layer is going to scale off during the following freeze/thaw cycle. The development of scaling
575 shown in figure 3 also supports this explanation. Here, for mixtures 033 and 044, the rate of scaling
576 seems to accelerate during periods, where the freezing chamber accidentally shut off. This may be
577 because there was longer time for the chemical degradation to develop between freeze/thaw cycles.

578

579 Two types of chemical surface degradation were briefly investigated by conducting salt frost
580 scaling tests for mixture 050EA in parallel to the standardized procedure described in section 2.7:

581

582 a. Leaching

583 b. Chemical reaction with de-icing salt

584

585 *a. Leaching (hydrolysis of the hardened paste)*

586 Calcium hydroxide has a relatively high solubility in water, compared to other hydration reaction
587 products. If the concrete is in contact with water, calcium hydroxide can be leached out. When the
588 calcium hydroxide is eliminated, other parts of the hardened cement paste will also start to
589 decompose [34]. In concrete with high contents of fly ash, the amount of calcium hydroxide in the
590 hardened cement paste is low. There are two reasons for this. First, less calcium hydroxide is
591 formed during cement hydration, because there is less cement from the beginning. Second, calcium
592 hydroxide formed during cement hydration is used during the pozzolanic reaction of the fly ash.
593 Therefore, in mixtures with high contents of fly ash less calcium hydroxide needs to be leached out
594 before other parts of the hardened cement paste starts to decompose, and therefore concrete with
595 high contents of fly ash may be more vulnerable to hydrolysis of the paste.

596

597 Rosenqvist [35] investigated the combined effect of leaching and frost action. In his experiments, he
598 studied the degradation occurring from leaching alone (without frost action) and the degradation
599 occurring during freezing and thawing (without leaching) as well as the degradation developing
600 during alternating leaching and frost action. His experimental results show that the combination of
601 leaching and freezing and thawing leads to more severe surface damage than the sum of damage
602 developed when one damage mechanism works at a time. This synergistic effect explains why
603 hydraulic structures in soft river water suffers from surface scaling, though concrete exposed to
604 freeze/thaw testing with pure water in the laboratory normally shows none or very limited scaling.
605 The difference is that the real structure is subject to leaching during summer, and then the degraded
606 surface layer scales off during the freeze/thaw cycles during winter. This does not happen in the
607 freeze/thaw test in the laboratory, where the solution in contact with the concrete surface is stagnant
608 (not flowing), and where there is shorter time for leaching to develop.

609

610 To investigate the combined action of leaching and freeze/thaw action, a freeze/thaw test was
611 conducted for mixture 050EA as described in section 2.7, but where the NaCl solution was changed
612 after every frost period (i.e. every 24 h) to intensify leaching. The experiment was stopped after 14
613 freeze/thaw cycles. There was no difference in scaling compared to the standard procedure, where
614 the freezing medium was changed after every 7 cycles.

615

616 *b. Chemical reaction with deicing salt*

617 If the surface is weakened by a chemical reaction with the deicing salt, then it is expected that the
618 degree of damage changes, if the deicing salt used in the standardized method is replace by another
619 deicing salt.

620

621 A freeze/thaw test as described in section 2.7 was carried out, but using CaCl_2 solution instead of
622 NaCl solution. The concentration of the CaCl_2 solution was adjusted, so the ion concentration was
623 identical to the 3% NaCl solution, so the freezing points of the two solutions were similar. After 56
624 freeze/thaw cycles, the amount of scaling for the test with CaCl_2 was 150% higher than the scaling
625 registered when using NaCl.

626

627 Based on this very preliminary study, it seems like the increased salt frost scaling observed for
628 concrete with a high content of fly ash is not due to combined action of leaching and
629 freezing/thawing. It may be due to a chemical reaction where chloride takes part, as the chloride
630 concentration in the CaCl_2 solution is higher than in the NaCl solution ($\text{Ca}:\text{Cl} = 1:2$; $\text{Na}:\text{Cl} = 1:1$).

631

632 Balonis et al. have described how chloride ingress changes the mineralogy of hardened cement
633 paste [36]. Their thermodynamic modelling is based on 25°C , not freezing temperatures, but it may
634 still be of relevance. In case of a binder based on pure Portland cement and a sufficiently high
635 chloride concentration, chloride will substitute sulfate in monosulfoaluminate ($\text{SO}_4\text{-AFm}$) and form
636 Freidel's salt (Cl-AFm). The liberated sulfate ions will react with more monosulfoaluminate and
637 calcium hydroxide to form ettringite (AFt). Seen in isolation, the transformation of $\text{SO}_4\text{-AFm}$ to
638 Cl-AFm reduces the volume of solid (calculated by using table values for molar volume in e.g.
639 [37]). However, this is more than compensated by the formation of ettringite, as this is an expansive
640 reaction, so the net effect of the chloride binding is a densification of the surface exposed to
641 chloride ingress. In the present study, the first exposure to chloride takes place 31 days after casting.
642 At this age, the amount of calcium hydroxide in the hardened cement paste is much lower for
643 mixtures containing fly ash than for the mixture without fly ash [38] (and also explained for

644 leaching). Due to the low content of calcium hydroxide in mixtures with fly ash, it is likely that the
645 transformation from $\text{SO}_4\text{-AFm}$ to Cl-AFm only to a very limited extent is followed by ettringite
646 formation, so in these cases the chloride binding will make the surface layer more porous. Balonis
647 et al. [36] have also described the change of phase distribution due to chloride exposure, if lime
648 stone filler is present in the binder. Here the carbonate during hydration is bound in
649 monocarboaluminate ($\text{CO}_3\text{-AFm}$). This AFm phase can also take part in ion exchange, so Cl-AFm
650 is formed during chloride ingress. The liberated carbonate will form calcite. CEM I cement is used
651 in the present study, so minimum 95% of the cement is clinker. However, the cement probably also
652 includes small amounts of limestone filler. Therefore, the carbonated layer as well as popcorn
653 calcite may have formed during the time of chloride exposure, and the carbonate originates from the
654 cement, not from atmospheric air. Both carbonation and popcorn calcite is also seen in samples
655 taken from marine structures below the average water level [39]. As such, the presence of popcorn
656 calcite is a sign of the change in mineralogy in the surface layer due to chloride ingress, and the
657 popcorn calcite is more likely to form in concrete with high contents of fly ash, because here the
658 concrete's content of calcium hydroxide is low. However, the presence of popcorn calcite may be
659 more than just a sign of chemical reaction. It may also be part of the problem with low salt frost
660 scaling resistance, as it increases the permeability of the surface layer [31].

661

662 The problem field of combined action that involves both chemical degradation and frost action calls
663 for more research. The classical frost attack is by nature a physical attack associated with the
664 transformation of liquid water to solid ice. If the frost attack is combined with a chemical attack, it
665 is necessary to understand the interplay with the paste matrix and how this interplay is influenced
666 by e.g. binder composition (more than just the physical strength of the paste). Suraneni et al. [40]
667 studied the formation of calcium oxychloride in concrete. It is an expansive reaction that involves

668 both calcium chloride, CaCl_2 , and calcium hydroxide, $\text{Ca}(\text{OH})_2$, as reactants. As CaCl_2 is often used
669 as de-icing chemical and as the calcium oxychloride formation is favored at low temperatures, the
670 chemical attack aggravates the salt frost scaling. Suraneni et al. [40] demonstrated that the use of fly
671 ash limits calcium oxychloride formation, because the pozzolanic reaction consumes the calcium
672 hydroxide formed during cement hydration, and then calcium hydroxide becomes in short supply
673 for the calcium oxychloride formation. However, the degree of cement substitution needs to be high
674 to effectively bring down the content of calcium hydroxide. Suraneni et al. have suggest 35%
675 cement substitution by fly ash, and even higher substitution levels may be necessary, depending on
676 the fly ash quality [41]. Suraneni et al. warn that the influence of high replacement levels on e.g.
677 salt frost scaling resistance needs to be investigated, before implementing high contents of fly ash as
678 a solution to the problem of calcium oxychloride formation. If the indications we have seen in our
679 laboratory are correct, this solution may cause other problems related to frost resistance.

680

681 **5. Conclusion**

682 This study demonstrates that when performing air void analysis on samples of hardened concrete,
683 e.g. according to the procedures described in ASTM C 457 and EN 480-11, then hollow fly ash
684 particles will show up as air voids. As the hollows in the fly ash particles are small, they do only to
685 a limited extent add to the registered total air content, but the presence of the hollow fly ash
686 particles may significantly change the measured spacing factor. The magnitude of the error
687 obviously depends on the amount of fly ash in the concrete mixture (as well as on the fly ash
688 quality). In the present study, air entrained concrete mixtures with $\text{FA}/(\text{C}+\text{FA})$ up to 50% were
689 tested. For the mixture with the highest fly ash content, the spacing factor was increased
690 approximately 25% when corrected for the presence of hollow fly ash particles.

691

692 The concrete mixtures have also been subjected to accelerated salt frost scaling testing. The
693 concrete mixtures all had comparable compressive strength and comparable air void characteristics,
694 when the correction for hollow fly ash particles had not been applied. For all concrete mixtures
695 except one, mixtures with higher contents of fly ash showed higher amounts of salt frost scaling (a
696 mixture with maximum dosage of fly ash and extra air entraining agent being the exception). The
697 difference in frost resistance between concrete with and without fly ash cannot be fully explained
698 by the distortion of the air void analyses due to the presence of hollow fly ash particles. The
699 corrected air void analyses point to that the critical spacing factor for mixtures with high contents of
700 fly ash is lower than 0.20 mm.

701

702 Though it was not part of the experimental plan to investigate the frost damage mechanism itself,
703 the experimental results indicate that for concrete mixtures with high contents of fly ash, there is a
704 combined effect of a chemical surface degradation and the physical frost attack.

705

706 **Acknowledgements**

707 The authors would like to acknowledge the sharing of results, access to human resources and
708 experimental facilities provided by the project "Green Transition of Cement and Concrete
709 Production" receiving financial support from the Danish Innovation Fond (InnovationsFonden).
710 Especially, Ulla Hjort Jakobsen, Danish Technological Institute, assisted with the petrographic
711 analyses.

712

713 During the review process, we received very detailed comments from the reviewer, as well as
714 references to related projects that we were not aware of. The contribution of the reviewer has both

715 helped to improve the present paper and been a source of inspiration for our future research related
716 to the frost resistance of concrete with high contents of fly ash. This effort is greatly acknowledged.

717

718 **References**

- 719 1. M. Thomas, *Optimizing the Use of Fly Ash in Concrete* (Portland Cement Association,
720 Publication IS548). [https://www.cement.org/docs/default-source/fc_concrete_technology/is548-](https://www.cement.org/docs/default-source/fc_concrete_technology/is548-optimizing-the-use-of-fly-ash-concrete.pdf)
721 [optimizing-the-use-of-fly-ash-concrete.pdf](https://www.cement.org/docs/default-source/fc_concrete_technology/is548-optimizing-the-use-of-fly-ash-concrete.pdf), 2007 (accessed 18 December 2018).
- 722 2. P. K. Mehta, High-performance, high-volume fly ash concrete for sustainable development, in:
723 Kejin Wang (Ed.), *Int. Workshop on Sustainable Development and Concrete Technology*,
724 Beijing, China, 2004, pp. 3-14.
- 725 3. T. Luping, I. Löfgren, *Evaluation of Durability of Concrete with Mineral Additions with regard*
726 *to Chloride-Induced Corrosion*, Chalmers University of Technology, Gothenburg, Sweden,
727 2016.
- 728 4. S.H. Gebler, P. Klieger, *Effect of fly ash on the durability of air-entrained concrete*, in: *Second*
729 *Int. Conf. Use Fly Ash, Silica Fume, Slag, Other Miner. By-Products Concr.* (ACI Spec. Publ.
730 SP-91), 1986: pp. 483–519.
- 731 5. T.R. Naik, R.N. Kraus, B.W. Ramme, Y.-M. Chun, *Deicing salt-scaling resistance: Laboratory*
732 *and field evaluation of concrete containing up to 70% Class C and Class F fly ash*, *J. ASTM Int.*
733 *2* (2005) 93–104. doi:10.1520/JAI11912.
- 734 6. K.H. Pedersen, A.D. Jensen, M.S. Skjøth-Rasmussen, K. Dam-Johansen, *A review of the*
735 *interference of carbon containing fly ash with air entrainment in concrete*, *Prog. Energy*
736 *Combust. Sci.* 34 (2008) 135–154. doi:10.1016/j.pecs.2007.03.002.
- 737 7. E. Siebel, *Air-void characteristics and freezing and thawing resistance of superplasticized air-*
738 *entrained concrete with high workability*, in: V. M. Malhotra (Ed.), *Third Int. Conf.*

- 739 Superplasticizers and Other Chemical Admixtures in Concrete, (ACI Spec. Publ. SP-119), 1989:
740 pp. 297–320.
- 741 8. N. Bouzoubaâ, A. Bilodeau, B. Fournier, R.D. Hooton, R. Gagné, M. Jolin, Deicing salt scaling
742 resistance of concrete incorporating supplementary cementing materials: laboratory and field
743 test data, *Can. J. Civ. Eng.* 35 (2008) 1261–1275. doi:10.1139/111-008.
- 744 9. E. Houehanou, R. Gagné, M. Jolin, Analysis of the representativeness and relative severity of
745 ASTM C672 and NQ 2621 900 standard procedures in evaluating concrete scaling resistance,
746 *Can. J. Civ. Eng.* 37 (2010) 1471–1482. doi:10.1139/L10-091.
- 747 10. D. Ehrhardt, Zum Einfluss der Nachbehandlung auf die Gefügeausbildung und den Frost-
748 Taumittelwiderstand der Betonrandzone (in German), Dr.-Ing Thesis, Bauhaus-Universität
749 Weimar, Germany, 2016.
- 750 11. M. Thomas, H. Yi, Deicer-salt scaling of concrete containing fly ash, in: M.T. Hasholt, F. Fridh,
751 R.D. Hooton (Eds.), *Int. RILEM Conf. Mater. Syst. Struct. Civ. Eng.*, RILEM Publications
752 S.A.R.L., Lyngby, Denmark, 2016: pp. 181–190.
- 753 12. D.P. Bentz, C.F. Ferraris, K.A. Snyder, Best practices guide for high-volume fly ash concretes:
754 Assuring properties and performance, NIST Technical Note 1812, Natl. Inst. Stand. Technol.,
755 Gaithersburg, 2013. doi:10.6028/NIST.TN.1812.
- 756 13. K.U. Christensen, Frost resistance of green concrete with high fly ash content, M.Sc. Thesis,
757 Technical University of Denmark, 2017.
- 758 14. DS 2426, Concrete – Materials – Rules for application of EN 206 in Denmark, Danish
759 Standards, 2013.
- 760 15. DS/EN 206-1, Concrete – Part 1: Specification, performance and conformity, Danish Standards,
761 2002.

- 762 16. DS/EN 197-1: Cement – Part 1: Composition, specifications and conformity criteria for
763 common cements, Danish Standards, 2012.
- 764 17. DS/EN 450-1: Cement – Part 1: Composition, specifications and conformity criteria for
765 common cements, Danish Standards, 2012.
- 766 18. W.R.L. da Silva, L.N. Thrane, T.L. Svensson, C. Pade, Performance-based design procedure for
767 the selection of concrete binder systems with low environmental impact, in: M.T. Hasholt (Ed.),
768 XXIII Nord. Concr. Research Symp., Aalborg, Denmark, 2017: pp. 23–26.
- 769 19. DS/EN 12350-2, Testing fresh concrete – Part 2: Slump-test, Danish Standards, 2012.
- 770 20. DS/EN 12350-7, Testing fresh concrete – Part 7: Air content – Pressure methods, Danish
771 Standards, 2012.
- 772 21. DS/EN 12390-3+AC, Testing hardened concrete – Part 3: Compressive strength of test
773 specimens, Danish Standards, 2012.
- 774 22. DS/EN480-11, Admixtures for concrete, mortar and grout – Part 11: Determination of air void
775 characteristics in hardened concrete, Danish Standards, 2005.
- 776 23. DS/CEN/TS 12390-9, Testing hardened concrete – Part 9: Freeze-thaw resistance – Scaling,
777 Danish Standards, 2006.
- 778 24. M. Pigeon and R. Pleau, Durability of concrete in cold climates, E & FN Spon, London, 1995.
- 779 25. G. Yıldırım, O. Öztürk, M. Şahmaran, M. Lachemi, Influence of ductility and microcracking on
780 the frost durability of cementitious composites with high volumes of fly ash, in: M.T. Hasholt,
781 K. Fridh, R.D. Hooton (Eds.), Int. RILEM Conf. Mater. Syst. Struct. Civ. Eng., RILEM
782 Publications S.A.R.L., Lyngby, Denmark, 2016: pp. 231–238.
- 783 26. J.J. Valenza, G.W. Scherer, A review of salt scaling: I. Phenomenology, Cem. Concr. Res. 37
784 (2007) 1007–1021. doi:10.1016/j.cemconres.2007.03.005.

- 785 27. A.A. Ramezaniapour, Effect of Curing on the Compressive Strength , Resistance to Chloride-
786 Ion Penetration and Porosity of Concretes Incorporating Slag , Fly Ash or Silica Fume, Cem.
787 Concr. Compos. 17 (1995) 125–133.
- 788 28. V.M. Malhotra, M.-H. Zhang, P.H. Read, J. Ryell, Long-Term Mechanical Properties and
789 Durability Characteristics of High-Strength/High-Performance Concrete Incorporating
790 Supplementary Cementing Materials under Outdoor Exposure Conditions, ACI Mater. J. 97
791 (2000) 518–525.
- 792 29. A. Vollpracht, M. Soutsos, F. Kanavaris, Strength development of GGBS and fly ash concretes
793 and applicability of fib model code’s maturity function – A critical review, Constr. Build.
794 Mater. 162 (2018) 830–846. doi:10.1016/j.conbuildmat.2017.12.054.
- 795 30. V. Penttala, Surface and internal deterioration of concrete due to saline and non-saline freeze-
796 thaw loads, Cem. Concr. Res. 36 (2006) 921–928. doi:10.1016/j.cemconres.2005.10.007.
- 797 31. A. Bilodeau, V. Sivasundaram, K.E. Painter, V.M. Malhotra, Durability of Concrete
798 Incorporating High Volumes of Fly Ash from Sources in the U.S., ACI Mater. J. 91 (1994) 3–
799 12.
- 800 32. N Thaulow, R.J. Lee, K. Wagner, S. Sahu, Effect of calcium hydroxide content on the form,
801 extent, and significance of carbonation, in: J. Skalny, J. Gebauer, I. Odler (Eds.), Material
802 Science of Concrete, Special Volume: Calcium Hydroxide in Concrete, The American Ceramic
803 Society, Westerville, OH, 2001, pp. 191–201.
- 804 33. B. Johannesson, P. Utgenannt, Microstructural changes caused by carbonation of cement
805 mortar, Cem. Concr. Res. 31 (2001) 925–931. doi:10.1016/S0008-8846(01)00498-7.
- 806 34. P.K. Mehta, P.J.M. Monteiro, Concrete. Microstructure, properties, and materials, fourth ed.,
807 McGraw-Hill Education, New York, 2014.

- 808 35. M. Rosenqvist, Frost-induced deterioration of concrete in hydraulic structures. Interaction
809 between water absorption, leaching and frost action, Doctoral Thesis, Report TVBM-1036,
810 Lund University, Sweden, 2016
- 811 36. M. Balonis, B. Lothenbach, G. Le Saout, F.P. Glasser, Impact of chloride on the mineralogy of
812 hydrated Portland cement systems, *Cem. Concr. Res.* 40 (2010) 1009–1022.
813 doi:10.1016/j.cemconres.2010.03.002.
- 814 37. B. Lothenbach, D.A. Kulik, T. Matschei, M. Balonis, L. Baquerizo, B.Z. Dilnesa, G.D. Miron,
815 M. R., Cemdata18: A chemical thermodynamic database for hydrated Portland cements and
816 alkali-activated materials., *Cem. Concr. Res.* 115 (2019) 472-506. doi:
817 10.1016/j.cemconres.2018.04.018.
- 818 38. F. Deschner, F. Winnefeld, B. Lothenbach, S. Seufert, P. Schwesig, S. Dittrich, F. Goetz-
819 Neunhoeffler, J. Neubauer, Hydration of Portland cement with high replacement by siliceous fly
820 ash, *Cem. Concr. Res.* 42 (2012) 1389–1400. doi:10.1016/j.cemconres.2012.06.009.
- 821 39. U.H. Jakobsen, K. De Weerd, M.R. Geiker, Elemental zonation in marine concrete, *Cem.*
822 *Concr. Res.* 85 (2016) 12–27. doi:10.1016/j.cemconres.2016.02.006.
- 823 40. P. Suraneni, V.J. Azad, O.B. Isgor, W.J. Weiss, Calcium oxychloride formation in pastes
824 containing supplementary cementitious materials: Thoughts on the role of cement and supple-
825 mentary cementitious materials reactivity, *RILEM Tech. Lett.* 1 (2016) 24–30.
826 doi:10.21809/rilemtechlett.2016.7.
- 827 41. P. Suraneni, V.J. Azad, O.B. Isgor, W.J. Weiss, Use of Fly Ash to Minimize Deicing Salt
828 Damage in Concrete Pavements, *Transp. Res. Rec. J. Transp. Res. Board.* 2629 (2017) 24–32.
829 doi:10.3141/2629-05.

830

831